Double-Diffusive Natural Convection with Marangoni and Cooling Effects

Norazam Arbin and Ishak Hashim

Abstract—Double-diffusive natural convection in an open top square cavity and heated from the side is studied numerically. Constant temperatures and concentration are imposed along the right and left walls while the heat balance at the surface is assumed to obey Newton's law of cooling. The finite difference method is used to solve the dimensionless governing equations. The numerical results are reported for the effect of Marangoni number, Biot number and Prandtl number on the contours of streamlines, temperature and concentration. The predicted results for the average Nusselt number and Sherwood number are presented for various parametric conditions. The parameters involved are as follows; the thermal Marangoni number, $0 \leq Ma_T \leq 1000$, the solutal Marangoni number, $0 \leq Ma_c \leq 1000$, the Biot number, $0 \leq Bi \leq 6$, Grashof number, $Gr = 10^5$ and aspect ratio 1. The study focused on both flows; thermal dominated, $N = 0.8$, and compositional dominated, $N = 1.3$.

Keywords—Double-diffusive, Marangoni effects, heat and mass transfer.

I. INTRODUCTION

THE flows generated by buoyancy due to simultaneous temperature and concentration gradients, also known as double diffusive convection, arises in a very wide range of fields such as oceanography, astrophysics, the process of chemical vapour transport, drying and crystal growth [1]. This type of flow have been studied experimentally and numerically, and also received considerable attention by many researchers.

Nishimura et al. [2] studied numerically double diffusive convection in a rectangular enclosure subject to opposing horizontal thermal and compositional buoyancies. They found that the oscillatory flow occurs in a limited range of buoyancy ratio. Costa [3] established the complete mathematical and numerical model for the calculation of double diffusive natural convection with heat and mass diffusive walls. The heat and masslines analysis were obtained in this study. The effect of magnetic field in the convection was then studied by Chamka & Al-Naser [4] and Teamah [5]. They obtained a good result and concluded that magnetic field will reduce the heat transfer and fluid circulation within the enclosure.

Bourich et al. [6] investigated the effect of buoyancy ratio on the dynamic behaviour of the fluid and heat and mass transfer for a double diffusive convection in a porous enclosure. Baytas et al. [7] showed that for a non-Darcy flow, where the enclosure filled with a step type porous layer, if the fluid/porous interface is not horizontal and contains a step change in height, the convection of the heat and mass are dramatically changed.

Most of the studies were done in closed rectangular or square cavities. Some of the recent researches were conducted by Li et al. [8], Chen et al. [9] and Teamah et al. [1]. Different enclosure geometries were studied by some researchers and good reviews were reported by Costa [10] and Papanicolaou & Belessiotis [11], where the enclosures are parallelogrammic and trapezoidal, respectively. The effect of Rayleigh number, the inclination angle and the aspect ratio of the enclosure will leave strong changes on the flow structure.

The problems of natural convection in an open cavity are starting to gain interest among researchers due to its wide application and involve Marangoni/surface tension effect. Sivasankaran et al. [12] studied numerically the magneto-convection of cold water in an open cavity with variable fluid properties. They observed that heat transfer rate behaves non-linearly with density inversion parameter and Marangoni number. Saleh et al. [13] investigated on the effect of cooling and surface tension on differentially heated open cavity. They concluded that global quantity of heat transfer rate decreases at the cold wall and increases at the hot wall with increasing cooling intensity for any fluid type.

Teamah & El-Maghlany [14] found that by increasing Lewis number, the mass transfer increased but there was no significant effect on the heat transfer for a case of double diffusive convection with insulated moving lid. The results of Younis et al. [15] on double diffusive natural convection in open lid enclosure filled with binary fluids, showed that the rate of heat and mass transfer are high for an enclosure with a free surface.

It is observed from the most studies available in the literature that double diffusive natural convection in open cavities with Marangoni effects have not been studied deeply. Therefore the aim of this work is to visualize and analyse Marangoni and convective cooling effects on a double diffusive natural convection in differentially heated open top square cavity.

Norazam Arbin is with the Department of Mathematics, Faculty of Computer and Mathematical Sciences, Universiti Teknologi Mara (Perak), 32610 Seri Iskandar, Perak, Malaysia (e-mail: noraz647@perak.uitm.edu.my).
Ishak Hashim is with the School of Mathematical Sciences, Faculty of Science and Technology, Universiti Kebangsaan Malaysia, 43600 Bangi Selangor, Malaysia (e-mail: ishak_h@ukm.my).

World Academy of Science, Engineering and Technology
International Journal of Physical and Mathematical Sciences
Vol:7, No:6, 2013

II. MATHEMATICAL FORMULATION

The schematic diagram of the system under consideration is shown in Fig. 1. Different temperature and concentrations were imposed between the left (T_c, c_c) and right walls (T_h, c_h), where $T_c < T_h$ and $c_c < c_h$. The bottom wall is adiabatic and impermeable. The top of the cavity is open and the temperature gradient is applied along the upper boundary. The heat balance at the upper boundary is assumed to obey Newton's law of cooling. Moreover, the top free surface is assumed to be insulating with respect to heat, non-diffusive with respect to the solute, flat and non-deformable, which means the surface tension is very high. The surface tension, σ, on the upper boundary is assumed to vary linearly with both T and c,

$$\sigma = \sigma_0 - \eta_T(T - T_0) - \eta_c(c - c_0) \tag{1}$$

where η_T and η_C are the thermal and solutal coefficients of surface tension, respectively. The Boussinesq approximation equation with opposite and compositional buoyancy force is used for the body force terms in the momentum equations, which is

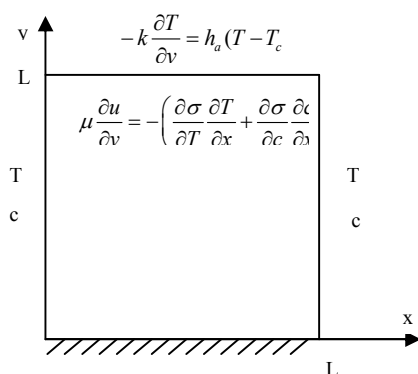$$\rho = \rho_0[1 - \beta_T(T - T_c) - \beta_c(c - c_c)] \tag{2}$$

Fig. 1 Schematic diagram of the model

The fluid is assumed to be Newtonian and incompressible. The flow is steady and laminar. The direction of the gravitational force is in the negative y-direction. Following the previous assumptions, the equations of mass, momentum, energy and concentration can be written in dimensional form as

$$\frac{\partial u}{\partial x} + \frac{\partial v}{\partial y} = 0 \tag{3}$$

$$u\frac{\partial u}{\partial x} + v\frac{\partial u}{\partial y} = -\frac{1}{\rho}\frac{\partial p}{\partial x} + \upsilon\left[\frac{\partial^2 u}{\partial x^2} + \frac{\partial^2 u}{\partial y^2}\right] \tag{4}$$

$$u\frac{\partial v}{\partial x} + v\frac{\partial v}{\partial y} = -\frac{1}{\rho}\frac{\partial p}{\partial y} + \upsilon\left[\frac{\partial^2 v}{\partial x^2} + \frac{\partial^2 v}{\partial y^2}\right] + g\beta_T(T - T_C) - g\beta_C(c - c_C) \tag{5}$$

$$u\frac{\partial T}{\partial x} + v\frac{\partial T}{\partial y} = \alpha\left[\frac{\partial^2 T}{\partial x^2} + \frac{\partial^2 T}{\partial y^2}\right] \tag{6}$$

$$u\frac{\partial c}{\partial x} + v\frac{\partial c}{\partial y} = D\left[\frac{\partial^2 c}{\partial x^2} + \frac{\partial^2 c}{\partial y^2}\right] \tag{7}$$

The boundary conditions are

$$u = v = 0, \; T = T_c \; and \; c = c_c \; at \; x = 0 \tag{8}$$

$$u = v = 0, \; T = T_h \; and \; c = c_h \; at \; x = L \tag{9}$$

$$u = v = 0, \; \frac{\partial T}{\partial y} = \frac{\partial c}{\partial y} = 0 \; at \; y = 0 \tag{10}$$

$$u = v = 0, \; -k\frac{\partial T}{\partial y} = h_a(T - T_c), \; \mu\frac{\partial u}{\partial y} = -\left(\frac{\partial \sigma}{\partial T}\frac{\partial T}{\partial x} + \frac{\partial \sigma}{\partial c}\frac{\partial c}{\partial x}\right) \; at \; y = L \tag{11}$$

Introducing the following non-dimensional variables for the governing equations,

$$X = \frac{x}{L}, \; Y = \frac{y}{L}, \; U = \frac{uL}{\alpha}, \; V = \frac{vL}{\alpha}, \; \Psi = \frac{\psi \Pr}{\upsilon}, \; \Omega = \frac{\omega L^2 \Pr}{\upsilon},$$

$$\Theta = \frac{T - T_c}{T_h - T_c}, \; C = \frac{c - c_c}{c_h - c_c}, \; \Pr = \frac{\upsilon}{\alpha}, \; Gr = \frac{\beta g(T_h - T_c)L^3}{\upsilon^2},$$

$$Ma_T = -\frac{\partial \sigma}{\partial T}\frac{(T_h - T_c)L}{\mu\alpha}, \; Ma_c = -\frac{\partial \sigma}{\partial T}\frac{(c_h - c_c)L}{D\mu}, \tag{12}$$

$$Bi = \frac{L/k}{1/h}, \; N = \frac{\beta_c(c_h - c_c)}{\beta_T(T_h - T_c)}$$

A set of governing equations in the stream function, vorticity and temperature is obtained after eliminating the pressure between the two momentum equations,

$$\frac{\partial^2 \Psi}{\partial X^2} + \frac{\partial^2 \Psi}{\partial Y^2} = -\Omega \tag{13}$$

$$\frac{\partial^2 \Omega}{\partial X^2} + \frac{\partial^2 \Omega}{\partial Y^2} = \frac{1}{\Pr}\left(\frac{\partial \Psi}{\partial Y}\frac{\partial \Omega}{\partial X} - \frac{\partial \Psi}{\partial X}\frac{\partial \Omega}{\partial Y}\right) - Gr\Pr\left(-\frac{\partial \Theta}{\partial X} + N\frac{\partial C}{\partial X}\right) \tag{14}$$

$$\frac{\partial^2 \Theta}{\partial X^2} + \frac{\partial^2 \Theta}{\partial Y^2} = \frac{\partial \Psi}{\partial Y}\frac{\partial \Theta}{\partial X} - \frac{\partial \Psi}{\partial X}\frac{\partial \Theta}{\partial Y} \tag{15}$$

$$\frac{\partial^2 C}{\partial X^2} + \frac{\partial^2 C}{\partial Y^2} = Le\left(\frac{\partial \Psi}{\partial Y}\frac{\partial C}{\partial X} - \frac{\partial \Psi}{\partial X}\frac{\partial C}{\partial Y}\right) \tag{16}$$

and the dimensionless boundary conditions are

$$\Psi = 0, \; \Omega = -\frac{\partial^2 \Psi}{\partial X^2}, \; \Theta = 0, \; C = 0 \; at \; X = 0 \tag{17}$$

$$\Psi = 0, \; \Omega = -\frac{\partial^2 \Psi}{\partial X^2}, \; \Theta = 1, \; C = 1 \; at \; X = 1 \tag{18}$$

$$\Psi = 0, \; \Omega = -\frac{\partial^2 \Psi}{\partial Y^2}, \; \frac{\partial \Theta}{\partial Y} = \frac{\partial C}{\partial Y} = 0 \; at \; Y = 0 \tag{19}$$

$$\Omega = -\left(Ma_T\frac{\partial \Theta}{\partial X} + \frac{Ma_c}{Le}\frac{\partial C}{\partial X}\right), \; \frac{\partial \Theta}{\partial Y} = Bi\Theta \; at \; Y = 1 \tag{20}$$

where the stream function, ψ, the vorticity, ω, the temperature, T, and the concentration, c, as variables are

World Academy of Science, Engineering and Technology
International Journal of Physical and Mathematical Sciences
Vol:7, No:6, 2013

defined as $u = \partial\psi/\partial y$, $v = -\partial\psi/\partial x$ and $\omega = (\partial v/\partial x) - (\partial u/\partial y)$.

A. Nusselt and Sherwood Number

The average Nusselt number that represents the total heat transfer across the enclosure is obtained by integrating the above local Nusselt number

$$\overline{Nu} = -\int_0^1 \left(\frac{\partial\Theta}{\partial X}\right)_{X=1} dY \qquad (21)$$

The average Sherwood number is obtained by integrating the above local Sherwood number

$$\overline{Sh} = -\int_0^1 \left(\frac{\partial C}{\partial X}\right)_{X=1} dY \qquad (22)$$

III. NUMERICAL METHOD AND VALIDATION

The governing equations (13) – (16) are solved by using the iterative finite difference method subject to the boundary conditions (17) – (20). The method of central difference is applied to discretizing the equations. The backward and forward different schemes are applied to the boundary conditions. A second order accurate formula is used for the vorticity boundary condition. The vorticity at the bottom wall is given as

$$\Omega = -\frac{(8\Psi_{1,j} - \Psi_{2,j})}{2(\Delta Y^2)} \qquad (23)$$

For the right and left walls, a similar formula is used. The algebraic equations are then solved by applying Gaussian SOR iteration. The unknown Ψ, Ω, Θ and C are calculated until the following criterium of convergence is satisfied

$$\frac{\sum_{i,j}\left|\zeta_{i,j}^{n+1} - \zeta_{i,j}^{n}\right|}{\sum_{i,j}\left|\zeta_{i,j}^{n+1}\right|} \leq \varepsilon \qquad (24)$$

where ζ is either Ψ, Ω, Θ and C. The iteration number and the convergence criterion are represented by n and ε, respectively. The integration of (21) and (22) is done by using the second order Simpson method. For the purpose of this study, the convergence criterion is set at $\varepsilon = 10^{-6}$. Regular and uniform grid distribution is used for the whole cavity. A grid resolution 120×120 is used for the simulation. For validation, the computed streamlines, isotherms and concentrations compare well with the results obtained by Chamka & Al-Naser [4] for $Pr = 1.0$, $Le = 2.0$, $Ra = 10^5$ and the aspect ratio is 2 as shown in Fig. 2. To further quantify the results, our average Nusselt number and Sherwood number compare well with that obtained by Chen et al. [16] as shown in Table I.
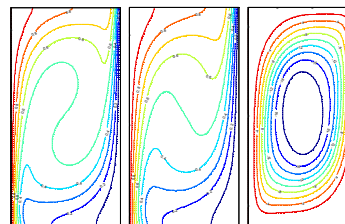

Fig. 2 Streamlines, isotherms and concentration for $Pr = 1.0$, $Le = 2.0$, $Ra = 10^5$ and $N = 0.8$

TABLE I
COMPARISON OF THE $\overline{Nu}$ AND $\overline{Sh}$ BETWEEN THE PRESENT AND THE RESULT OF [16] FOR $Ra = 10^5$, $Pr = 1.0$ AND $Le = 2.0$.

		[16]	Present
N=0.8	$\overline{Nu}$	3.6897	3.7311
	$\overline{Sh}$	4.9156	4.9074
N=1.3	$\overline{Nu}$	2.1255	2.401
	$\overline{Sh}$	3.1615	3.2365

IV. RESULT AND DISCUSSION

The parameters involved in this investigation are as follows; the thermal Marangoni number, $0 \leq Ma_T \leq 1000$, the solutal Marangoni number, $0 \leq Ma_c \leq 1000$, the Biot number, $0 \leq Bi \leq 6$, Grashof number, $Gr = 10^5$ and aspect ratio 1. For the purpose of this study the same value for thermal and solutal Marangoni numbers are used for all cases. In addition, the results for the average Nusselt number, $\overline{Nu}$, and average Sherwood number, $\overline{Sh}$, for various conditions will be presented.

Fig. 3 presents the contours of streamlines, temperature and concentration for the thermal dominated flow where $Pr = 0.054$, $Bi = 1$ and various thermal and solutal Marangoni number. A large counter clockwise rotating cell occurs in the core of the cavity due to the temperature difference between the hot (right) and cold (left) walls. The cells are beginning to change its form into smaller size when the shear stress is imposed to the free surface as shown in Fig. 3 (b). It indicates that the buoyancy force starting to decrease and no longer dominating the fluid motion. The concentration contours are starting to distort at the free surface of the enclosure. By increasing the Marangoni number (Ma_T and Ma_c) up to 600, the fluid motion become slower and a clockwise streamline cells become focused at the upper right corner while the contours of isotherms and concentration tend to become more similar.

The effect of Marangoni to the fluid flow, temperature and concentration for the compositional dominated flow is shown in Fig. 4. Without the presence of the surface tension ($Ma_T = Ma_c = 0$), a large rotating streamline cells exist at the core where similar contours occurs for the isotherms and concentrations. When the thermal and solutal Marangoni


numbers getting higher, the large cells become distorted to the upper right corner of the surface and develop more rotating cells. What more interesting, the velocity of the fluid flow is increased. The value of Ψ_{max} indicates that the streamline is proportional to both Marangoni effects. The isotherms and concentrations are almost parallel to each other and drive toward the hot wall when the Marangoni number increased.

Fig. 5 shows the Nusselt and Sherwood number as a function of Marangoni number for different values of Biot number. Without the presence of convective cooling ($Bi = 0$), the values of $\overline{Nu}$ and $\overline{Sh}$ are gradually decreased in the beginning but started to increase for some high Marangoni number ($Ma > 600$) at $N = 0.8$. This differs from high Bi where the heat and mass transfer being suppressed as Ma takes higher value. An increasing patterns is observed for Fig. 5 (b) where $N = 1.3$. The strong convective cooling do influenced the efficiency of the heat and mass transfer rate across the cavity. The transfer rate for both ($\overline{Nu}$ and $\overline{Sh}$) values are more consistent for high Biot number ($Bi = 6$). This fact is due to the external convection resistance decreased and causes the improvement of both transfer rates especially at the upper right corner of the cavity.

V. Conclusion

This present work has focused on double diffusive natural convection with Marangoni and cooling effects in a differentially heated square cavity. The characteristics of the streamlines, isotherms and concentration for various Biot number, thermal and solutal Marangoni number were investigated and analyzed. The study revealed the following:

1) The fluid flow, temperature and concentration distribution within the cavity depended on the surface tension, convective cooling and buoyancy ratio (thermal or compositional).

2) The heat and mass transfer mechanism are strongly depended on buoyancy ratio where the compositional dominated flow made the transfer rates more efficient for considered conditions.

3) For N = 0.8, the $\overline{Nu}$ and $\overline{Sh}$ displays a similar trends of decreasing except at Bi = 0. The presence of convective cooling will suppressed the heat and mass transfer rates. A contrary phenomena occurs for N = 1.3, where the $\overline{Nu}$ and $\overline{Sh}$ number increased gradually for all Biot numbers.
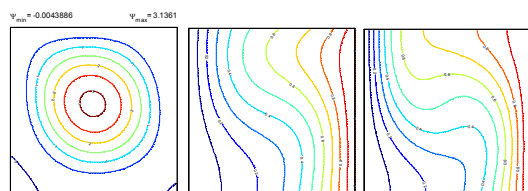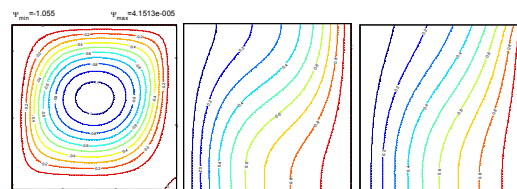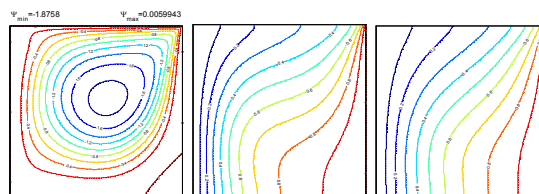

(a) $Ma_T = Ma_c = 0$
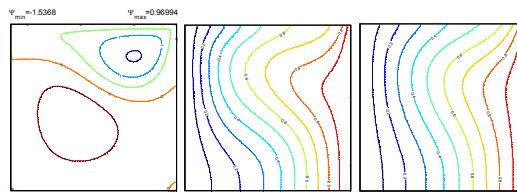
(b) $Ma_T = Ma_c = 600$

Fig. 3 Streamlines, isotherms and concentration for $Pr = 0.054$, $Bi = 1$, $N = 0.8$ and various Marangoni number

(a) $Ma_T = Ma_c = 0$

(b) $Ma_T = Ma_c = 600$

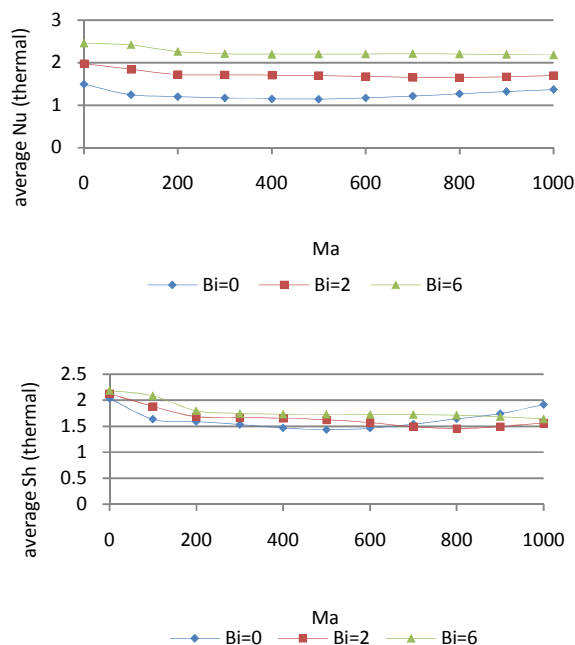Fig. 4 Streamlines, isotherms and concentration for $Pr = 0.054$, $Bi = 1$, $N = 1.3$ and various Marangoni number

Fig. 5 (a) Average Nusselt number and Sherwood number ($N = 0.8$) vs Marangoni number, $\left(Ma_T = Ma_c\right)$ for various Biot number
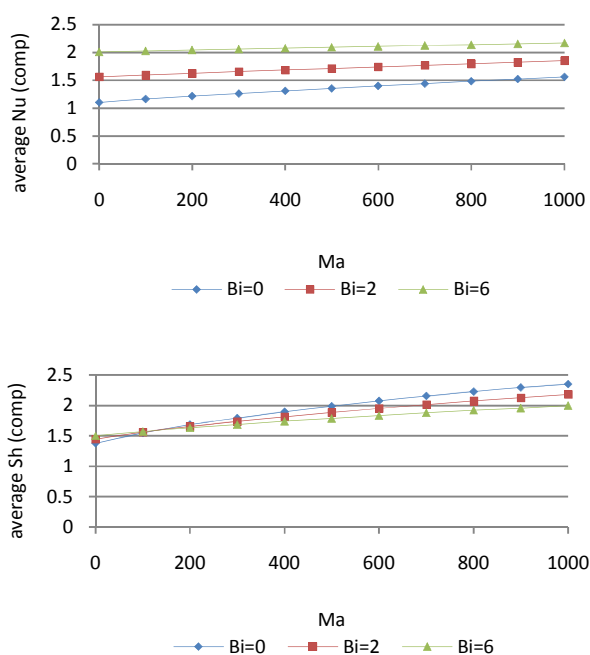
World Academy of Science, Engineering and Technology
International Journal of Physical and Mathematical Sciences
Vol:7, No:6, 2013

World Academy of Science, Engineering and Technology
International Journal of Physical and Mathematical Sciences
Vol:7, No:6, 2013

Fig. 5 (b) Average Nusselt number and Sherwood number ($N = 1.3$) vs Marangoni number, $\left(Ma_T = Ma_c \right)$ for various Biot number

REFERENCES

[1] M. A. Teamah, A. F. Elsafty, E. Z. Massoud, Numerical simulation of double diffusive natural convective flow in an inclined rectangular enclosure in the presence of magnetic field and heat source, Int. J. Thermal Sciences, Vol. 52, p. 161-175, 2012.

[2] T. Nishimura, M. Wakamatsu, A. M. Morega, Oscillatory double-diffusive convection in a rectangular enclosure with combined horizontal temperature and concentration gradients, Int. J. Heat Mass Transfer, Vol. 41, p. 1601-1611, 1998.

[3] V. A. F. Costa, Double diffusive natural convection in a square enclosure with heat and mass diffusive walls, Int. J. Heat Mass Transfer, Vol. 40, p. 4061-4071, 1997.

[4] A. J. Chamka, H. Al-Naser, Hydromagnetic double-diffusive convection in a rectangular enclosure with opposing temperature and concentration gradients, Int. J. Heat Mass Transfer, Vol. 45, p. 2465-2483, 2002.

[5] M. A. Teamah, Numerical simulation of double diffusive natural convection in rectangular enclosure in the presence of magnetic field and heat source, Int. J. Thermal Sciences, Vol. 47, p. 237-248, 2008.

[6] M. Bourich, A. Amahmid, M. Hasnaoui, Double diffusive convection in a porous enclosure submitted to cross gradients of temperature and concentration, Energy Conversion and Management, Vol. 45, p. 1655-1670, 2004.

[7] A. C. Baytas, A. F. Baytas, D. B. Ingham, I. Pop, Double diffusive natural convection in an enclosure filled with a step type porous layer: Non-Darcy flow, Int. J. Heat Thermal Sciences, Vol. 48, p. 665-673, 2009.

[8] Y. Li, Z. Chen, J. Zhan, Double-diffusive Marangoni convection in a rectangular cavity: Transition to chaos, Int. J. Heat Mass Transfer, Vol. 53, p. 5223-5231, 2010.

[9] C. F. Chen, C. L. Chan, Stability of buoyancy and surface tension driven convection in a horizontal double-diffusive fluid layer, Int. J. Heat Mass Transfer, Vol. 53, p. 1563-1569, 2010.

[10] V. A. F. Costa, Double-diffusive natural convection in parallelogrammic enclosures, Int. J. Heat Mass Transfer, Vol. 47, p. 2913-2926, 2004.

[11] E. Papanicolaou, V. Belessiotis, Double-diffusive natural convection in an asymmetric trapezoidal enclosure: unsteady behaviour in the laminar and the turbulent-flow regime, Int. J. Heat Mass Transfer, Vol. 48, p. 191-209, 2005.

[12] S. Sivasankaran, M. Bhuwaneswari, Y. J. Kim, C. J. Ho, K. L. Pan, Numerical study on magneto-convection of cold water in an open cavity with variable fluid properties, Int. J. Heat and Fluid Flow, Vol. 32, p. 932-942, 2011.

[13] H. Saleh, N. Arbin, R. Roslan, I. Hashim, Visualization and analysis of surface tension and cooling effects on differentially heated cavity using heatline concept, Int. J. Heat Mass Transfer, Vol. 55, p. 6000-6009, 2012.

[14] M. A. Teamah, W. M. El-Maghlany, Numerical simulation of double-diffusive mixed convection flow in rectangular enclosure with insulated moving lid, Int. J. Thermal Sciences, Vol. 49, p. 1625-1638, 2010.

[15] L. B. Younis, A. A. Mohamad, A. K. Mojtabi, Double diffusion natural convection in open lid enclosure filled with binary fluids, Int. J. Thermal Sciences, Vol. 46, p. 112-117, 2007.

[16] S. Chen, J. Tolke, M. Krafczyk, Numerical investigation of double-diffusive (natural) convection in vertical annuluses with opposing temperature and concentration gradients, Int. J. Heat and Fluid Flow, Vol. 31, p. 217-226, 2010.